RGNZ/MGPB

The analysis of wellbore instability based on the Hoek-Brown failure criterion using geomechanical units and discontinuities evaluation

Rudarsko-geološko-naftni zbornik
(The Mining-Geology-Petroleum Engineering Bulletin)
DOI: 10.17794/rgn.2026.1.13

Original scientific paper

Mohamadali Chamanzad[1], Majid Nikkhah[1]*, Ahmad Ramezanzadeh[1], Misha Pezeshki[2], Imandokht Mostafavi[2]

[1] *Faculty of Mining, Petroleum & Geophysics Engineering, Shahrood University of Technology, Shahrood, Iran.*

[2] *Pars Oil and Gas Company, Iran.*

Abstract

The accuracy of wellbore instability assessment becomes reliable when sufficient geomechanical model data and appropriate failure criteria parameters are used. The Hoek-Brown failure criterion is widely used in wellbore instability analysis; however, limited focus has been given to parameter determination and the specific conditions for its application (intact rock or rock mass) within wells. In this study, theoretical wellbore analysis was conducted using various failure criteria, with a primary focus on comparing the Hoek-Brown criterion for both intact rock and rock mass conditions. A geomechanical model was developed using petrophysical logs, laboratory tests, and downhole measurements. The geomechanical units of the wellbore were determined through clustering algorithms, supported by downhole plugs. Natural discontinuities within the wellbore were identified using image logs, and their distribution was mapped for each geomechanical unit. The parameters for intact rock in the Hoek-Brown criterion were derived from laboratory test results, while those for the rock mass condition were determined using the rock mass rating (RMR) and geological strength index (GSI). The results indicate that applying the Hoek-Brown criterion assuming intact rock does not provide a reliable estimation of wellbore instability. However, by using the criterion under rock mass conditions, wellbore failures can be accurately predicted according to the wellbore conditions. Additionally, evaluating the wellbore conditions based on geomechanical units improves the theoretical analysis's accuracy and identifies stable and unstable zones.

Keywords:
Hoek-Brown criterion; geomechanical unit; rock mass classification; wellbore instability

1. Introduction

The economic loss caused by wellbore instability worldwide exceeds one billion dollars annually (**Zeynali, 2012**), accounting for over 40% of non-productive wellbore time (**Zhang et al., 2009**). In one of the wells located in southwest Iran, instability led to a 51-day drilling suspension, resulting in an estimated loss of $2,550,000 (**Abdideh & Navadeh Tayyebi, 2020**). Hydrocarbon wells play a critical role in the extraction of oil and gas, essential resources for global energy needs. With increasing demand, wells are often drilled in close proximity to each other, in complex geological formations, or in challenging environments. This proximity and complexity can raise concerns regarding wellbore stability, which is crucial for safe and efficient resource extraction.

Understanding the mechanical behaviour of formations is further complicated by the fact that rocks in nature are rarely ideal or uniform. A Discontinuous, Inhomogeneous, Anisotropic, Non-Elastic (DIANE) rock is the material with which the engineer has to deal. There is a connection between each of the characteristics of discontinuousness, inhomogeneity, anisotropy and non-elasticity (**Hudson & Harrison, 2000**). Wellbore instability analysis can be conducted under different assumptions, such as Non-elastic behaviour (**Garavand et al., 2020**), the presence of discontinuities in intact rocks (**Jamshidi & Amani, 2014**), and account for heterogeneity (**Wang et al., 2023**) and anisotropy (**Asaka & Holt, 2021**), thus offering a more realistic representation of rock behaviour.

Depending on the problem type, available data, and specific objectives, a suitable modelling approach is selected – often neglecting the simultaneous consideration of all these factors. Investigating each of these characteristics individually or collectively is a fundamental challenge in addressing geomechanical and wellbore stability problems. For instance, the role of discontinuities and anisotropy in shale formations has been emphasized in various studies (**Ostadhassan, 2016**). Similarly, the behaviour of fractured reservoirs has been modelled using non-elastic approaches to account for the mechanical

* Corresponding author: Majid Nikkhah
e-mail address: madjid.nikkhah@gmail.com
Received: 2 March 2025. Accepted: 20 September 2025.
Available online: 2 January 2026

effects of discontinuities (**Mehrabian, 2016**). The application of uncertainty modelling has also been explored to assess wellbore stability in heterogeneous formations (**Agheshlui & Matthai, 2017**).

However, most studies either assume intact rock or incorporate limited fracture information in wellbore stability assessments (**Kang et al., 2009**), and the use of rock mass assumptions for wellbore instability analysis has not been commonly practiced. In this study, the Hoek–Brown failure criterion is used to compare intact rock and rock mass conditions in wellbore stability analysis. Discontinuities and fractures were identified to estimate rock mass parameters, and geomechanical units were constructed to reflect the heterogeneity observed in the wellbore. For intact rock conditions, the modelling assumed isotropic mechanical properties, no fractures, and an elasto-plastic constitutive law, whereas for the rock mass condition, heterogeneity and discontinuities were incorporated through zonation and strength index calibration.

2. Literature Review

For well design, the initial analysis of wellbore instability is generally performed based on data from drilled wells and evaluated using empirical methods (**Zadravec & Krištafor, 2018**). Subsequently, the most suitable solutions, empirical methods, and recommendations are applied for the design of subsequent wells. Failure criteria are among the most significant parameters influencing analysis and design. The Hoek-Brown failure criterion, with its unique structure, has gained attention as a widely used criterion in geomechnical issues, such as cavern stability (**Suchowerska et al., 2012**), rock slope stability (**Yang et al., 2004**), and tunnel design (**Jearsiripongkul et al., 2022**).

2.1. Failure mechanism in wellbore instability

Wellbore instability can arise from four main causes: mechanical (shear and tensile failures), structural (e.g. weak formations with weak layering), drilling-induced issues, and chemical reactions between the drilling fluid and the formation (**Pašić et al., 2007**). The accurate selection of an appropriate failure criterion that accounts for these causes – especially mechanical failures and geological structure – is crucial for aligning the analysis with real wellbore conditions. Furthermore, considering the influence of the parameters used in the criterion can enhance the alignment between the analysis and actual wellbore conditions (**Rahimi & Nygaard, 2018**).

2.2. Hoek-Brown criteria

The Hoek-Brown failure criterion, known for its comprehensive framework incorporating both the strength properties of intact rock and geological observations, is one of the most widely used criteria for rock mass-related challenges (**Rafiei Renani & Cai, 2022**). The Hoek-Brown failure criterion introduced in the early 1980s, as shown in **Equation 1**, this criterion was designed to predict the strength limits of intact rock and rock mass. In this equation, the parameters represent s as the rock integrity, while m is a constant dependent on the rock type (**Brown & Hoek, 1980**).

Despite the common practice of determining intact rock properties through laboratory tests, estimating geological features, particularly for rock mass, presents significant challenges (**Wei et al., 2020**). Several relationships have been proposed to estimate the m and s parameters within the Hoek-Brown criterion. For example, **Zuo et al. (2008)** developed a method based on crack propagation theory, while **Wei et al. (2020)** introduced relationships involving uniaxial compressive strength and fracture characteristics.

Additionally, the estimation of the parameters m and s based on two classification indices, rock mass rating (RMR'_{76}) (**Hoek & Brown, 1988**) and geological strength index (GSI) (**Hoek, 1994**), has been proposed and revised, as shown in **Equations 2** and **3** (**Hoek & Brown, 2019**). These relationships have been employed by various researchers in different fields, including wellbore stability (**Elyasi & Goshtasbi, 2015; Ma et al., 2018; Yamashiro et al., 2018**). The optimal value for m_i in this equation is determined based on the best fit of the failure envelope drawn from laboratory data and the value of D (the damage factor) depending on the drilling used.

Various methods have been proposed to determine the values of GSI and RMR, though the approach for determining GSI and RMR in wellbore stability studies has received less attention. The GSI classification was initially introduced qualitatively based on the visual structure of the rock mass, and subsequently, many methods for its quantitative determination were proposed (**Yang & Elmo, 2022**). **Kang et al. (2017)** introduced a method based on the average spacing of discontinuities and the surface condition index of the discontinuities, which was also utilized in this study. The RMR classification (**Bienawski, 1976**) were modified to this classification to provide more reliable estimates of the Hoek-Brown criterion parameters using this classification (**Hoek & Brown, 1988**). The use of Hoek-Brown criterion in wellbore instability analysis has also been significant, although in some cases, this application has occurred without adequate attention to the methods and importance of determining the parameters of this criterion.

2.2.1. Hoek-Brown criterion Equations

The Hoek-Brown failure criterion is formulated as follows (**Brown & Hoek, 1980**):

$$\sigma_1 = \sigma_3 + (m\sigma_c\sigma_3 + s\sigma_c^2)^a \quad (1)$$

Where:

σ_1 – major principal stress (MPa),

σ_3 – minor principal stress (MPa),

m – material constant dependent on rock type,

s – rock integrity parameter,

σ_c – uniaxial compressive strength (MPa).

The parameters m and s are estimated using the following relationships (**Hoek, 1994; Hoek & Brown, 1988**):

$$m = m_i \exp\left(\frac{(GSI\ or RMR'_{76}) - 100}{28 - 14D}\right) \quad (2)$$

$$s = \exp\left(\frac{(GSI or RMR'_{76}) - 100}{9 - 3D}\right) \quad (3)$$

Where:

m_i – initial material constant,

GSI – Geological Strength Index,

RMR'76 – Rock Mass Rating (1976),

D – damage factor.

2.2.2. Other Criteria equation

The remaining failure criteria for intact rock conditions have been compared with the Hoek-Brown criterion, as presented in **Table 1**.

2.3. Previous studies

Researchers have widely applied the Hoek-Brown criterion in the analysis of wellbore instability, often comparing it with other criteria. For instance, in studies where wellbore stability was modelled, this criterion has frequently shown better alignment with actual wellbore conditions compared to the Mohr-Coulomb model, though exceptions exist. **Zhang et al. (2010)** suggested using the Hoek-Brown criterion with assumed parameters for intact rock, alongside the Mogi-Coulomb criterion, to predict the safe mud weight window.

Further studies, such as **Gholami et al. (2014)**, have evaluated the Hoek-Brown, Mohr-Coulomb, and Mogi-Coulomb failure criteria in designing safe mud weight windows for wells from carbonate reservoirs in the southwest of Iran. Their research found that the Mogi-Coulomb criterion exhibited better agreement with wellbore observations, recommending it for safe mud weight design. Although, the assumptions about intact rock versus rock mass and the Hoek-Brown criterion parameters were not fully addressed in this study.

Similarly, **Rahimi and Nygaard (2015)** examined thirteen different failure criteria for safe mud weight de-

Table 1. Rock failure criteria equations

Failure criteria	Governing equation	Refrences	Eq
Mohr–Coulomb	$\sigma_1 = \sigma_c + \frac{1+\sin\varphi}{1-\sin\varphi}\sigma_3$	(Jaeger et al., 2007)	(4)
Stasi Dalia	$J_2 = \frac{(\sigma_c - \sigma_t)I_1 + \sigma_c\sigma_t}{3}$	(Stassi-D'Alia, 1967)	(5)
Mogi Columb	$\tau_{oct} = a + b\sigma'_{m,2}$	(Al-Ajmi & Zimmerman, 2005)	(6)
$a = \frac{2\sqrt{2}}{3}C\cos\varphi,\ b = \frac{2\sqrt{2}}{3}\sin\varphi$			
Inscribed Drucker-Prager	$\sqrt{J_2} = a + \frac{bI_1}{3}$	(Veeken et al., 1989)	(7)
$a = \frac{3\sigma_c\cos\varphi}{2\sqrt{q}\sqrt{9+3\sin\varphi^2}},\ b = \frac{3\sin\varphi}{\sqrt{9+3\sin\varphi^2}},\ I_1 = \sigma_1 + \sigma_2 + \sigma_3$			
Circumscribed Drucker-Prager	$\sqrt{J_2} = a + \frac{bI_1}{3}$	(Zhou, 1994)	(8)
$a = \frac{\sqrt{3}\sigma_c}{2+q},\ b = \frac{\sqrt{3}(q-1)}{2+q}$			
Modified Lade	$\frac{I_1^{"3}}{I_3^{"}} = 27 + \eta$	(Ewy, 1999)	(9)
$I_1^{"} = (\sigma_1 + S) + (\sigma_2 + S) + (\sigma_3 + S),\ I_3^{"} = (\sigma_1 + S) + (\sigma_2 + S) + (\sigma_3 + S),\ \eta = \frac{4tg\varphi^2(9 - 7\sin\varphi)}{(1-\sin\varphi)},\ S = \frac{C}{tg\varphi}$			

σ_1 – Maximum principal stress (MPa), σ_2 – Intermediate principal stress (MPa), σ_3 – Minimum principal stress (MPa), σ_c – Uniaxial compressive strength (MPa), σ_t – Tensile strength (MPa), C – Rock cohesion (MPa), φ – Internal friction angle (°), J_2 – Second stress invariant (MPa²), I_1 – First stress invariant (MPa), τ_{oct} – Octahedral shear stress (MPa), $\sigma'_{m,2}$ – Mean effective stress (MPa), S – Strength parameter (MPa), q – Drucker-Prager coefficient, η – Failure criterion parameter.

termination in shale, sandstone, and siltstone formations. Their findings suggested that the Stassi-D'Alia, modified Griffith, and Hoek-Brown criteria were more sensitive to variations in rock mechanical parameters, making them less suitable. **Ma et al. (2018)** used both the Hoek-Brown (assuming rock mass) and Mohr-Coulomb criteria in a numerical model to assess wellbore instability across three stress regimes. Their findings revealed that the failure zone predicted by the Hoek-Brown criterion was larger than that of the Mohr-Coulomb model, requiring higher mud pressure for stability, highlighting the importance of correctly estimating the m and s parameters.

More recent research by **Lakirouhani et al. (2021)** compared the Hoek-Brown and Fairhurst failure criteria on laboratory samples of granite and marble. The samples (and the parameters) were in intact rock and the results show that both criteria provided acceptable outcomes. **Abazari et al. (2022)** utilized three criteria – Hoek-Brown, Mohr-Coulomb, and Mogi-Coulomb – to evaluate the failures of a wellbore in the carbonate oil field of Kopal. In this study, the GSI index was used to estimate the parameters for the Hoek-Brown criterion under rock mass conditions. As a result, the Hoek-Brown criterion gave an intermediate limit between the other two criteria.

3. Solution method

In this study, the most appropriate methods for constructing the geomechanical model were introduced and applied based on laboratory and wellbore test results in one of the Persian Gulf carbonate reservoirs. Subsequently, the geomechanical units (GMUs) were identified from petrophysical logs using three clustering approaches – hierarchical clustering (with various metric and linkage criteria), density-based clustering, and k-means – and were then evaluated using core test results and the silhouette index. The parameters related to the RMR and GSI indices for the rock mass were determined based on the interpretation of image logs and the identification and evaluation of wellbore discontinuities, separately for each geomechanical unit (GMU). The parameters m and s in the Hoek-Brown failure criterion were estimated for both intact rock – based on laboratory test results (m_i) – and rock mass conditions based on two classification systems, RMR'_{76} and GSI. These estimations were performed separately for each geomechanical unit (GMU) and also as an overall evaluation for the entire wellbore. Theoretical wellbore analysis using the Hoek–Brown criterion was first conducted under intact rock conditions. In two scenarios – based on estimated parameters for each geomechanical unit and for the entire wellbore – the results were compared with six failure criteria: Mohr–Coulomb, Stasi–Dalia, Mogi–Coulomb, Inscribed Drucker–Prager, Circumscribed Drucker–Prager, and Modified Lade. Finally, theoretical wellbore analysis using the Hoek–Brown criterion for rock mass conditions was performed under four scenarios (1) using RMR values for each geomechanical unit (HB-RG), (2) using a single RMR value for the entire wellbore (HB-RT), (3) using GSI values for each geomechanical unit (HB-GG), and (4) using a single GSI value for the entire wellbore (HB-GT). These results were compared and evaluated against the two previous scenarios based on intact rock conditions.

4. Case Study

The wellbore under analysis is located in a field on the shared border between Iran and one of the Arab countries. This field is situated in the Coastal Fars geological zone and has an anticlinal structure. Structurally, it is a domal and uplifted structure, with the main cause of the uplift being the rise of the Qatar-Fars arch (**Klemme, 1984**). The information analyzed pertains to two formations: the Kangan and Dalan formations, where the Kangan Formation belongs to the Early Triassic period, and the Dalan Formation dates back to the Permian period. The Kangan Formation (Lower to Middle Triassic) and the Upper Dalan Formation (Upper Permian) are equivalent to the Khuff Formation, consisting of a carbonate-evaporite sequence overlying the anhydrites of the Nar Formation. The Kangan and Dalan formations are divided into sections K1 to K4 based on reservoir properties, with their stratigraphic column shown in **Figure 1** (**Tavakoli, 2015**).

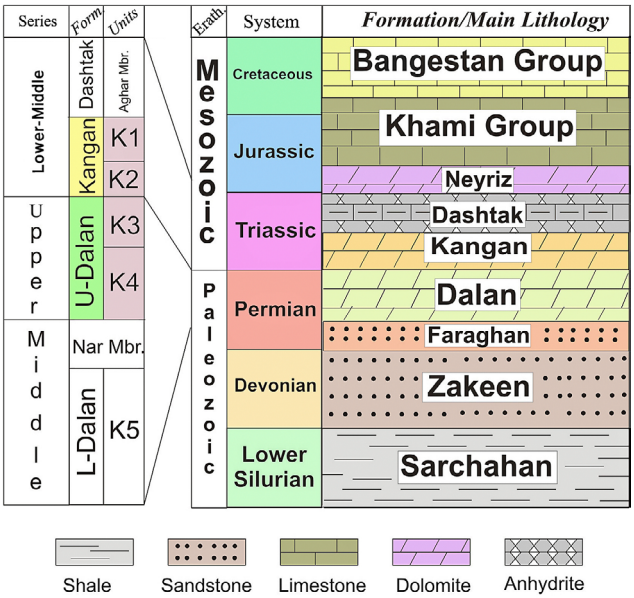

Figure 1. Stratigraphic Column in the Central Part of the Persian Gulf (**Tavakoli et al., 2018**)

4.1. Geomechanical Model

Building the geomechanical model and identifying the key parameters for assessing wellbore stability is the

Table 2. Average Results of Density, Triaxial, and Uniaxial Tests on Plugs.

GMU	Density (gm/cm³)	UCS (MPa)	Friction Angle (degree)	Young's modulus (Gpa)	Poisson's ratio
V	2.66	145.7	-	44.0	-
X	2.56	116.5	30.8	34.8	0.28
Y	2.26	42.0	15.0	15.1	0.24
Z	2.01	22.4	11.1	10.7	0.26

first step in wellbore analysis. **Abdollahipour et al. (2019)**, categorized the key parameters influencing wellbore stability for both soft and hard rock types based on the results of numerical model analysis. Their research shows that for soft rock (with an average Young's modulus of 5 GPa), the most important factors are in-situ stress, pore pressure, internal friction angle, Young's modulus, and cohesion. For hard rock (with an average Young's modulus of 15 GPa), the most critical factors are in-situ stress, drilling fluid pressure, and Young's modulus, respectively.

The constructed geomechanical model typically includes the elastic properties of rocks, such as elastic modulus, Poisson's ratio, and strength parameters like compressive strength, cohesion, and internal friction angle. Additionally, other critical elements of a geomechanical model are variations in pore pressure and the in-situ stress conditions of the region being studied (**Zoback, 2010**). The dynamic Young's modulus and Poisson's ratio were estimated as the first step in constructing the geomechanical model.

Many relationships have been proposed for estimating uniaxial compressive strength, Poisson's ratio, Young's modulus, and static Poisson's ratio for carbonate rocks. Most of them were evaluated in this study for use in constructing the geomechanical model. Ultimately, empirical relationships were selected based on the carbonate origin of the wellbore and laboratory results. To improve the reliability and precision of the geomechanical model, core plug data were thoroughly used for calibration and were integrated into each geomechanical unit.

Most of the core plugs within each GMU were taken at very close intervals, which greatly contributed to the uniformity and homogeneity of the plugs and the results for each category. A total of 25 uniaxial and triaxial compressive strength tests were conducted, with 11 of them being uniaxial tests. The characteristics of the samples and a summary of the tests performed are presented in **Table 2**. The results of the triaxial tests were also used to estimate uniaxial compressive strength and for calibration along the wellbore path. Testing could not be conducted on samples from the W geomechanical unit due to a shortage of specimens, so its values were estimated using petrophysical logs and calibrated based on other results. The test results show that the internal friction angle for X, Y, and Z geomechanical units is 30.8°, 15.0°, and 11.1°, respectively, while the cohesion values are 30.7 MPa, 18.4 MPa, and 11.4 MPa, respectively.

The pore pressure was estimated using an equation provided by **Azadpour et al. (2015)** for a gas field in the Persian Gulf. Since the MDT (Modular Formation Dynamics Tester) test was conducted at certain points in the well, the estimated value was refined using the MDT results. In this equation, the total porosity is derived from the logs, and the effective stress is calculated as the difference between the total stress gradient and the hydrostatic pressure gradient (10.5 MPa/km). The constant γ' was proposed to be 0.96 for the gas reservoir.

The in-situ stress state was determined using borehole breakouts and field leak-off tests. In this well, the FMI (Formation Micro-Imager) log was used to identify breakouts and estimate the direction of the in-situ stress. The results from the image log and the bedding orientations indicate that the overburden stress is one of the principal stresses. Based on the shear and tensile failures observed within the well, the maximum and minimum horizontal stress directions were estimated to be 40° and 130°, respectively.

For building the geomechanical model in this wellbore, the poroelasticity relationships were used to estimate the horizontal stress. Estimating these stresses requires an approximation of the tectonic strains and a trial-and-error solution. Other parameters in these equations, such as Young's modulus, Poisson's ratio, pore pressure, and vertical stress, had been estimated in previous stages.

4.1.1. Geomechanic's Equations

Here are the equations for Dynamic Young's modulus and Poisson's ratio given in **Equations 10** and **11** as follows (**Fjaer et al., 2008**):

$$E_{dyn} = \rho V_s^2 \left(\frac{3V_p^2 - 4V_s^2}{V_p^2 - V_s^2}\right) \tag{10}$$

$$\upsilon_{dyn} = \frac{V_p^2 - 2V_s^2}{2(V_p^2 - V_s^2)} \tag{11}$$

Where:

E_{dyn} – dynamic Young's modulus (GPa),
υ_{dyn} – dynamic Poissins's ratio,
ρ – density (kg/m³),
V_p – compressional wave velocities (m/s),
V_s – shear wave velocities (m/s).

Empirical relationships **12** through **15** respectively were selected for an estimation of static Young's modulus (**Aboutaleb et al., 2018**), static Poisson's ratio (**Ane-**

mangely et al., 2019), uniaxial compressive strength (**Farquhar et al., 1994**), and friction angle (**Edimann et al., 1998**) based on the carbonate origin of the wellbore and laboratory results.

$$E_s = -31.23 + 131.5\nu_{dyn} + 0.45E_{dyn} \quad (12)$$

$$\nu_s = \nu_{dyn} \quad (13)$$

$$UCS = 174.8exp(-0.093n) \quad (14)$$

$$\varphi = 41.92 - 0.7779n \quad (15)$$

Where:

Es – static Young's modulus (GPa),
υ_s – static Poissins's ratio,
UCS – uniaxial compressive strength (MPa),
φ – friction angle (degree),
n – porosity (%).

The pore pressure gradient estimation equation (**Azadpour et al., 2015**):

$$P_{Pg} = \left(\frac{(1-\varnothing)\sigma_{eff}}{1-2\varnothing}\right)^{\gamma} \quad (16)$$

Where:

P_{Pg} – static Young's modulus (GPa),
Ø – total porosity (fraction),
σ_{eff} – difference between the total stress gradient and the hydrostatic pressure gradient (MPa/km),
γ' – proposed to be 0.96 for the gas reservoir.

The overburden stress and horizontal stress estimation using relationships (**Fjaer et al., 2008**):

$$S_V = \rho_W g Z_W + \int_{Z_W}^{Z} \rho(z) g dZ \approx \rho_W g(Z_W + (Z - Z_W)) \quad (17)$$

$$S_h = \frac{\upsilon}{1-\upsilon}(S_V - \alpha P_P) + \alpha P_P + \frac{E}{1-\upsilon^2}(\varepsilon_h + \upsilon\varepsilon_H) \quad (18)$$

$$S_H = \frac{\upsilon}{1-\upsilon}(S_V - \alpha P_P) + \alpha P_P + \frac{E}{1-\upsilon^2}(\varepsilon_H + \upsilon\varepsilon_h) \quad (19)$$

Where:

S_V – overburden stress (MPa),
ρ_W – water density (kg/m^3),
Z_W – water depth (m),
ρ(z) – overburden density (kg/m^3),
Z – overburden depth (m),
g – gravity (m/s^2),
S_h – minimum horizontal stress (MPa),
S_H – maximum horizontal stress (MPa),
P_p – Pore pressure (MPa),
α – Biot's coefficient,
ε_h – minimum tectonic strain,
ε_H – maximum tectonic strain.

4.2. Geomechanical Units

Defining geomechanical units alongside a geomechanical model aids in better understanding geomechanical variations within the wellbore and helps analyze related geological issues. For example, constructing a geomechanical model and identifying five GMUs in a wellbore from the Persian Gulf reservoirs aimed at determining optimal drilling parameters (such as direction and angle) and creating stable conditions for each identified geomechanical unit (**Kadkhodaie, 2021**). Geomechanical units are often defined in studies based on petrophysical logs, seismic data, apparent rock indices, engineering judgment, or intelligent clustering methods. **Mehrgini et al. (2016)** identified geomechanical unit boundaries using compressional and shear sonic logs, density, and neutron porosity logs, relying on engineering-based interpretation. Subsequently, five geomechanical units were distinguished, and thin section analysis was performed using three samples per meter to evaluate their microscopic features. **Nazari Sarem and Riahi (2020)** identified geomechanical units in the Mansouri field using seismic data and Multiresolution Graph-based Clustering. **Gharechelou et al. (2022)** visually defined five geomechanical units for a carbonate formation in southwest Iran based on apparent plug characteristics, including mineral composition, microscopic features, visual porosity, cementation, and dolomitization. **Pourreza et al. (2023)** applied hierarchical clustering using shear sonic log data to identify geomechanical units. **Ruiz and Batezelli (2024)** classified a Brazilian field using a K-means clustering approach based on laboratory measurements, wellbore data, logs, and thin section analyses. **Al-Kaabi et al. (2024)** employed and compared three methods – graph-based clustering, self-organizing maps (SOM), and hierarchical clustering – to identify geomechanical units in the Kangan and Dalan formations.

The geomechanical units in this study were determined based on petrophysical logs using various clustering algorithms. The output was evaluated using core plug samples and the silhouette index for each clustering method. The advantage of determining geomechanical units using log data is that the same method can be applied to other wells when the log data is available. The dynamic Young's modulus and Poisson's ratio were determined using **Equations 10** and **11** to compare the geomechanical units.

The log data, including density, neutron, gamma, compressional and shear sonic logs in the 8.5-inch borehole, were fully utilized, and the statistical analysis of the data was conducted in the same interval. Five logs – density, neutron, gamma, compressional and shear sonic logs – were used for classification. The mineral log was not directly considered in this classification, and the gamma log was employed as a guide for lithology variations. Three logs – density, compressional, and shear sonic logs – were selected as parameters related to the sample behaviour in the equations. Porosity, being an important factor in rock behaviour (**Dalirnasab et al., 2024**), was also considered to improve the consistency

between the defined geomechanical units and the core plug samples.

To help determine the appropriate number of geomechanical units, 38 mm diameter core plugs were first classified into five categories using non-destructive measurements based on rock type, porosity, and permeability. The purpose of this classification was to use the sample's depth for calibrating and evaluating the accuracy of geomechanical units. However, placing samples into distinct category came with challenges, especially for plugs located near the boundary of two units. Significant differences in porosity and permeability were observed between some plugs taken from the same depth. In such cases, the plugs were categorized based on the results of strength tests. Accordingly, with the help of depth and rock type logs, the initial classification of the plugs into five categories was made, as shown in **Figure 2**. Samples in Category 1 (Z's GMU) had the highest porosity, while Categories 4 and 5 (W and V GMUs) exhibited the lowest porosity. The fifth plug category showed porosity comparable to Category 4, but differed in mineral composition and permeability, as identified through the logs. Additionally, Categories 2 and 3 (X's and Y's GMUs) were considered intermediate groups. They had similar permeability values, while Category 3 displayed lower porosity. The distinguishing factor between Categories 3 and 4 was the difference in their porosity. Therefore, five geomechanical units were assumed in this study based on the classification of the plugs and the distribution of log data.

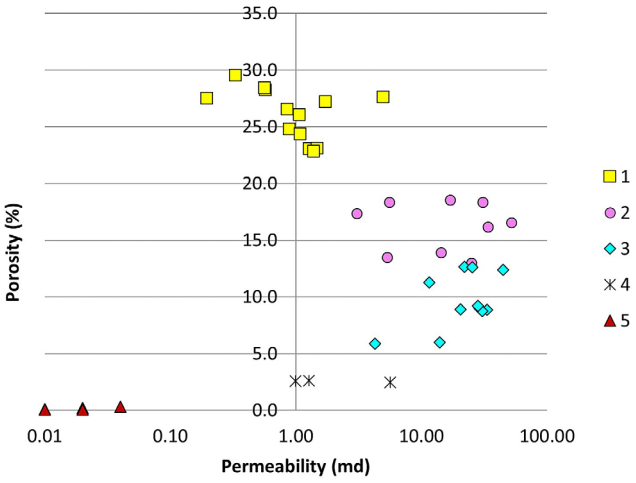

Figure 2. Classification of core plug samples based on measured porosity and permeability

Determining geomechanical units in the wellbore is challenging due to the high volume of petrophysical data and the limited core information. Using clustering algorithms helps reduce engineering and visual interpretation errors. Three clustering methods – hierarchical clustering, density-based clustering, and K-means – were used in this study for GMU clustering. In the hierarchical method, it is necessary to determine the distance between two data points as well as the distance between two sets (clusters of data). The distance between two data points is evaluated using a distance metric, while the distance between two sets is assessed using a linkage criterion (**Abbas, 2008**). Euclidean distance that depicts the distance between two points based on the Pythagoras theorem is one of the most utilized algorithms in the cluster investigation (**Prakash, 2024**). The density-based method defines a cluster as a continuous region in the data space with high point density, separated from other clusters by regions with low point density. Data points in these separating regions, with lower density, are usually considered noise. It requires two input parameters: the neighbourhood radius (rn) and the minimum number of points (MinPts) needed to form a dense region. The K-means method, a popular approach, aims to divide the data into number of clusters, where each data point belongs to the cluster with the nearest mean. A key input parameter is the number of clusters (K), which must be specified in advance (**Hasan et al., 2023**).

The number of geomechanical units was set to five based on our plug analysis, and this value served as the primary input for methods requiring a predefined cluster count. For the density-based approach, we determined rn = 0.42 and MinPts = 5 by inspecting k-distance plots to capture the most coherent high-density regions while filtering out noise. In the hierarchical method, various distance metric, including Euclidean distance, squared Euclidean distance, and standardized Euclidean distance, along with different linkage criteria for set distance, such as average, centroid, complete, single, median, Ward's minimum variance algorithm, and weighted averaging. The resulting dendrogram was then cut to yield five final clusters. Finally, for K-means, we set K = 5 and ran the algorithm multiple times with different random initial centroids to ensure consistent clustering results.

The best clustering method was determined based on the division of plugs in **Figure 2** and the silhouette index, which ranges from -1 (least match) to +1 (best match). The silhouette score measures how similar an object is to its own cluster (cohesion) compared to other clusters (separation). If most objects have high silhouette values, the clustering structure is appropriate. However, if many points have low or negative values, it indicates that the clustering structure may have too many or too few clusters.

The match between the clustering results and the plug classification, in terms of percentage, as wellbore as the silhouette index for all three clustering methods, is presented in **Table 3**. A higher match percentage between the clustering results and the plug classification indicates a more accurate clustering method, and a higher silhouette index indicates greater precision of the clustering method. The match percentage and silhouette index for hierarchical clustering methods are higher than for the K-means and density-based methods. Additionally, the

Table 3. Percentage of agreement between clustering results and plug classification and silhouette index

Density-based		42%,-0.56						
K-means		79%,0.38						
Hierarchical		**Linkage criterion**						
		average	centroid	complete	median	single	ward	weight
Metric	Euclidean	76%,0.35	61%,0.48	82%,0.48	76%,0.31	39%,0.21)	94%,0.45	85%,0.47
	Squared Euclidean	73%,0.49	85%,0.46	82%,0.48	76%,0.38	39%,0.21	70%,0.49	85%,0.38
	Standardized Euclidean	58%,0.44	79%,0.45	61%,0.41	73%,0.35	39%,0.21	94%,0.48	91%,0.44

Table 4. Average Log Values for the Five Geomechanical Units in the Well

GMU	**Lithology**	**Frequency (%)**	**PHIE log**		**E dyn (Gpa)**		***v* dyn**	
			Ave	**SD**	**Ave**	**SD**	**Ave**	**SD**
V	Dolomite	22	0.02	0.01	90.1	6.0	0.26	0.01
W	Limestone	15	0.04	0.03	69.0	8.3	0.28	0.03
X	Limestone	14	0.06	0.03	72.4	5.5	0.27	0.03
Y	Dolomite	29	0.12	0.03	53.2	5.8	0.26	0.03
Z	Limestone	20	0.18	0.04	41.2	6.1	0.25	0.02

silhouette index for hierarchical clustering with the linkage criteria "single," "median," and "average" is the lowest. The results using the standardized Euclidean distance metric were better compared to the Euclidean and squared Euclidean. The standardized Euclidean method with the Ward linkage algorithm produced the best results and was used in this study.

The frequency of the five geomechanical units along the wellbore and the average log values of porosity, Young's modulus, and dynamic Poisson's ratio for each GMU can be observed in **Table 4**. The geomechanical units exhibit differences in various aspects, which validate the significance of the proposed classification. The distribution of geomechanical units in the well, along with the variations in stress parameters, pore pressure, uniaxial compressive strength, internal friction angle, and cohesion, is illustrated in **Figure 3**.

4.3. Rock mass condition

The condition and distribution of discontinuities were evaluated to determine the rock mass condition and assign scores to the classification indices. In order to evaluate the discontinuities within the well, their distribution and density in each GMU, and to apply the results to the Hoek-Brown failure criterion, the discontinuities within the wellbore were identified. The use of image logs for breakout geometry and detecting active faults has also been highlighted in recent studies (**Heydari Gholanlo & Nikkhah, 2023**). The number and types of discontinuities were determined using resistivity image logs. In this method, bright colors in the logs indicate low conductivity and high resistance, which signify low porosity and permeability, while discontinuities are displayed in dark colors. The way the discontinuity plane intersects with the wellbore is identified as perpendicular (circular image), angled (elliptical image), or parallel to the wellbore (two parallel lines along the wellbore axis), with the corresponding image appearing as horizontal, sinusoidal, or vertical on the log, as shown in **Figure 4**.

Discontinuities within the wellbore have been categorized for analysis into three groups: primary natural, secondary natural, and failures due to instability. Primary natural discontinuities include bedding planes, which are identified by color changes within the image log and generally exhibit permeability and aperture similar to the host rock. Secondary natural discontinuities include stylolites (serrated, wavy lines), lamination, open fractures, and cracks within the wellbore, which typically have higher permeability compared to the host rock.

The GMU for each data point in the wellbore (approximately every 15 cm) was identified in the previous section, with the total number of data points for each GMU corresponding to its total recognized length. The percentage of natural discontinuities relative to the total data points for each GMU is shown in **Figure 5**. According to this figure, approximately 60% of the length of Z geomechanical unit is associated with discontinuities, while 40% is discontinuity-free. Excluding open fractures, the percentage of discontinuities decreases as the mechanical strength of the geomechanical units increases (from Z to V). Lamination, bedding, and other discontinuities are more prevalent in geomechanical units with weaker mechanical properties. As shown, open fractures have a high percentage in V geomechanical unit, which has higher rock strength. Given the low porosity of this unit, the formation of open fractures was possible. Stylolites are absent in geomechanical units with either very low or very high mechanical strength.

The values of GSI and RMR were used to estimate *m* and *s*, which were determined based on the discontinuity

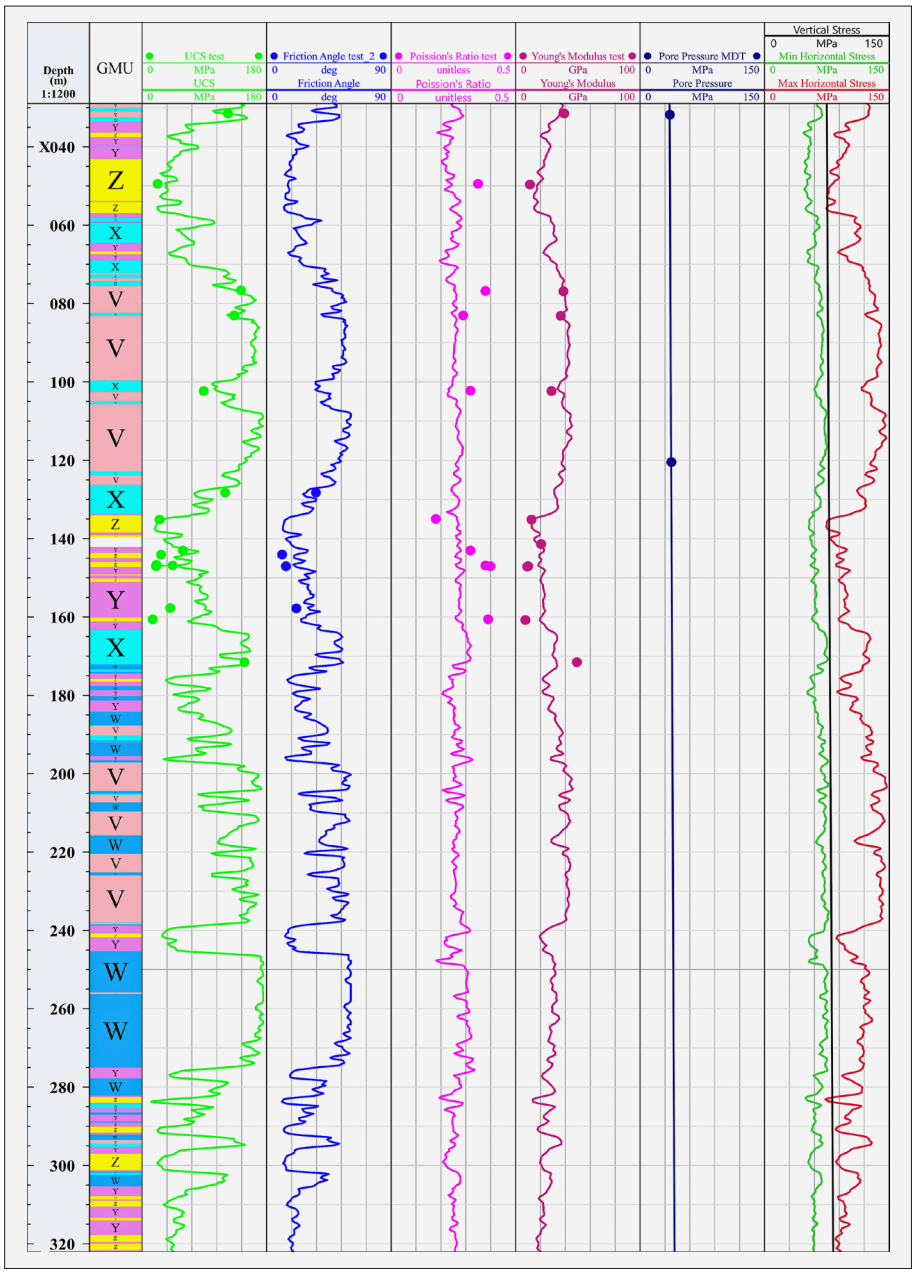

Figure 3. Geomechanical Units and Changes in Geomechanical Parameters Along the Well

conditions evaluated earlier. The GSI value was estimated based on the average spacing of discontinuities and the surface condition index of the discontinuities, following the method provided by **Kang et al. (2017)**. The RMR classification was also calculated RMR modifications (**Hoek & Brown, 1988**) and was based on six parameters: uniaxial compressive strength (UCS), RQD index, discontinuity spacing, discontinuity condition, groundwater, and orientation of discontinuities.

The parameters m and s were estimated based on GSI and RMR values for the entire wellbore and for each geomechanical unit separately, as shown in **Table 5**. As mentioned, the m_i value was determined based on the strength parameters, such as the internal friction angle, and the best-fit failure envelope from laboratory data. The RMR values obtained for the geomechanical units were generally higher than the GSI values, except in the W geomechanical unit, where GSI was higher. This was due to the sensitivity of the method used, influenced by the spacing of discontinuities and the low number of discontinuities in this unit. Finally, wellbore instability was evaluated using the m and s values obtained from these two rock mass classification systems.

5. Wellbore Instability Analysis

The theoretical analytical model used in this study was solved under the assumption of elasticity, and it does not account for inelastic behaviour or thermo-hydro-mechanical coupling effects. The theoretical analysis of wellbore instability has been conducted using various failure criteria for each data point (every 15 cen-

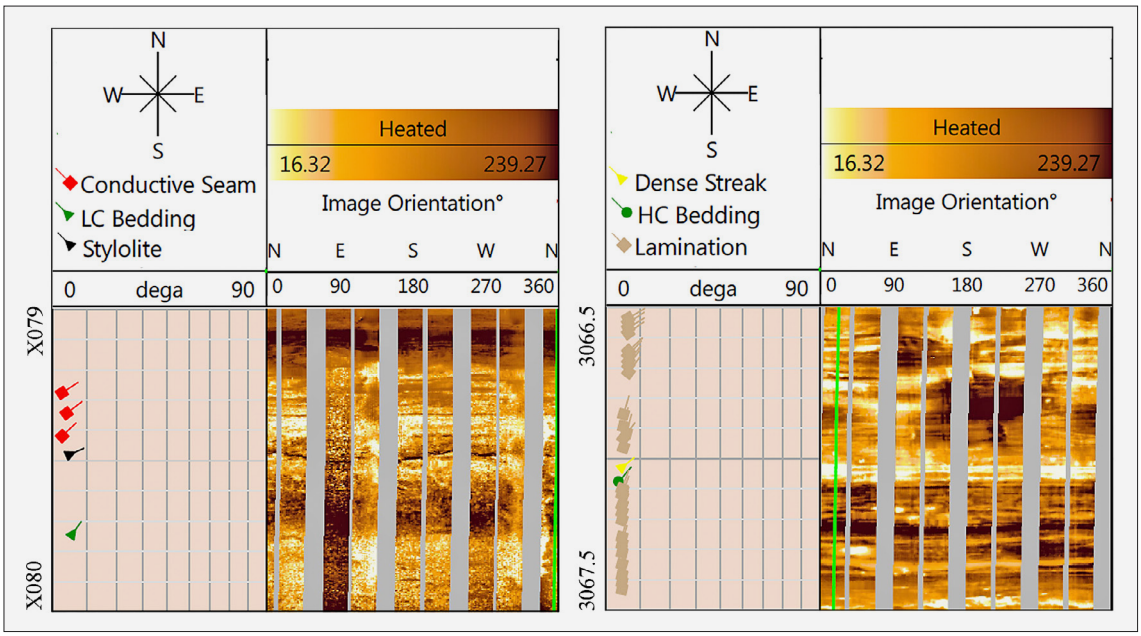

Figure 4. An example of discontinuities observed in the image log

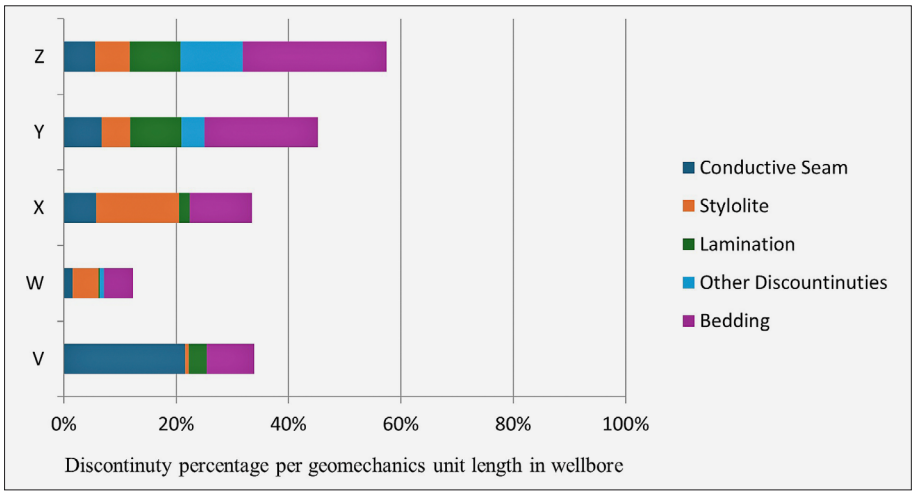

Figure 5. Frequency percent of different types of discontinuities relative to the total length of each GMU

timeters of 290 meters) from the well. In fact, the modelling was performed in two dimensions for each section of the wellbore, where the in-situ stresses were considered anisotropic, while mechanical parameters such as elastic modulus were assumed to be isotropic, which is a common assumption for carbonate formations. The evaluation of wellbore failures was initially conducted using the Hoek-Brown failure criterion, assuming intact rock conditions in the wellbore. The results were then compared with six other criteria: Mohr-Coulomb, Modified Lade, Stassi D'Alia, Mogi-Coulomb, and both the inscribed and circumscribed Drucker-Prager criteria.

The theoretical analysis, based on the outcome of each criterion for each point along the well, compared to the actual wellbore conditions, are shown in **Figure 6**. The theoretical analysis of each data point of the wellbore was predicted as either stable or unstable by each failure criterion, and the results were compared with the actual conditions in the wellbore (stable or unstable), as shown in the figure. If a point in the wellbore was identified as stable by the theoretical analysis and was also stable based on the image logs, it is displayed in dark green. If a point was identified as unstable by the theoretical analysis and also unstable according to the image

Table 5. Estimation of m and s values for the Hoek-Brown criterion using RMR and GSI

GMU	m_i	RMR	m	s	GSI	m	s
V	44	82	23.3	0.14	76	18.7	0.07
W	40	82	20.8	0.13	85	23.4	0.19
X	35	79	16.3	0.09	73	13.1	0.05
Y	14	74	6.6	0.05	68	5.4	0.03
Z	10	72	4.3	0.04	65	3.4	0.02
Totally (Average)	35	77	13.6	0.08	75	12.6	0.06

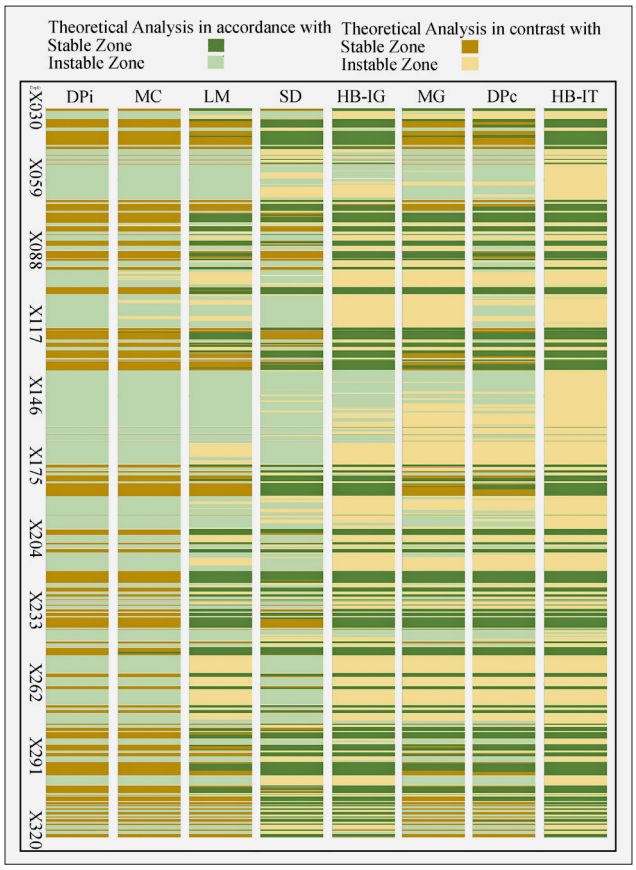

Figure 6. Performance of Failure Criteria Against Observed Conditions in the Well

logs, it is displayed in light green. If a point was identified as stable but predicted as unstable by the theoretical analysis, it is shown in dark gold, and if a point was identified as unstable but predicted as stable by the theoretical analysis, it is shown in light gold.

For example, the theoretical analysis of the Mohr-Coulomb and inscribed Drucker-Prager failure criteria predicted most of the points in the wellbore as unstable, which contrasts with the stable points (dark gold) and aligns with the unstable points in the wellbore (light green). The Stassi D'Alia criterion had the highest alignment with the stable and unstable points in the well, while the inscribed and circumscribed Drucker-Prager criteria acted as upper and lower bounds for predicting wellbore conditions.

6. Results

The use of the Hoek-Brown criterion under intact rock conditions, assuming a single value of m_i for the entire well (HB-IT) and a value of m_i for each geomechanical unit (HB-IG), has led to two different results. As shown in **Figure 7**, under the HB-IT condition, all points in the wellbore were predicted as stable, but when m_i was assigned for each geomechanical unit, the match between the Hoek-Brown failure criterion and the actual wellbore conditions significantly improved. Quantitatively, the percentage of alignment for the HB-IT and HB-IG methods across the entire wellbore (the ratio of green points to total wellbore points) was 37.5% and 49.6%, respectively. As observed, using specific values for each geomechanical unit (HB-IG) improved the accuracy of the Hoek-Brown failure criterion for evaluating wellbore conditions under intact rock.

The evaluation of the results obtained from the analysis of well conditions for different values of m and s in both intact and rock mass scenarios (RMR and GSI) is shown in **Figure 7**. The methods include assumptions of intact rock with uniform parameter values across the entire well (HB-IT), intact rock with parameter values spe-

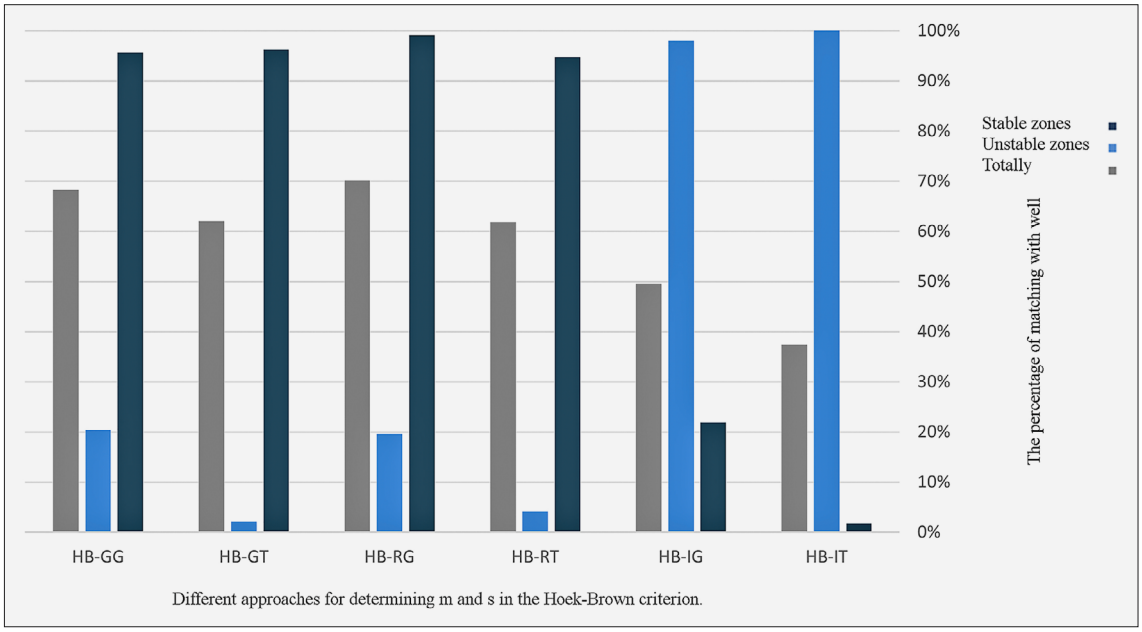

Figure 7. Correspondence between predicted failures and actual in-wellbore conditions for different methods.

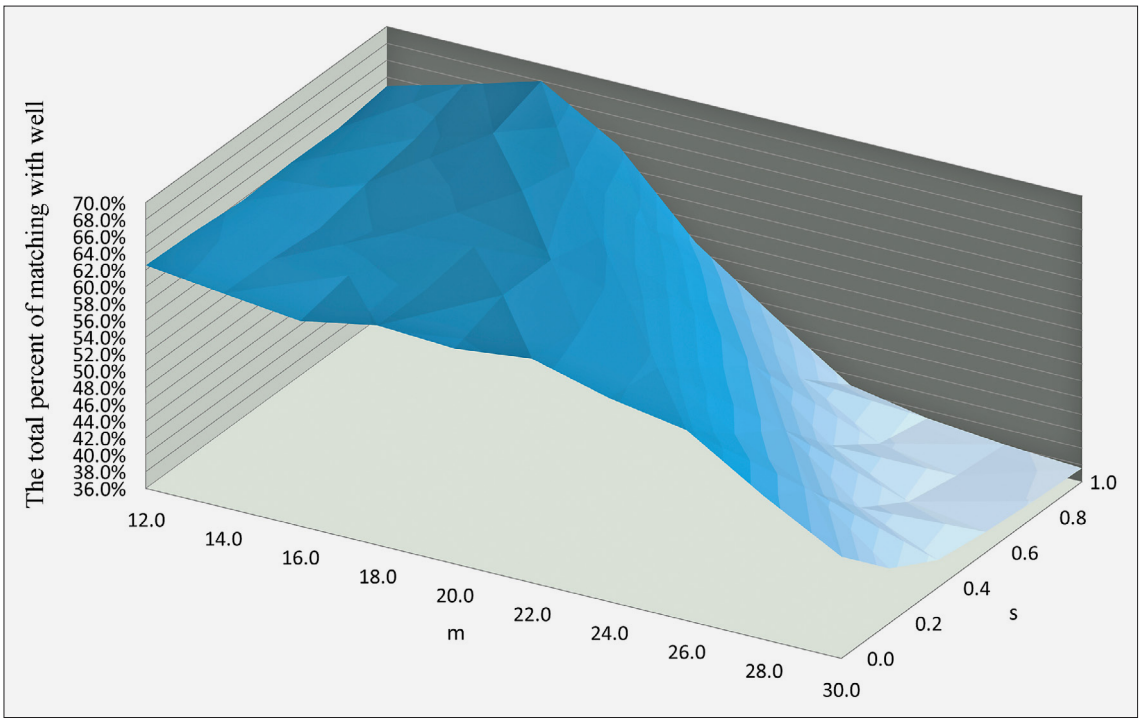

Figure 8. Back analysis for values of m and s based on the percentage of match between predicted conditions and actual in-wellbore observations

cific to each geomechanical unit (HB-IG), rock mass with parameter values from RMR and uniform across the entire well (HB-RT), rock mass with parameter values from RMR and specific to each geomechanical unit (HB-GT), rock mass with parameter values from GSI and uniform across the entire well (HB-GI), and rock mass with parameter values from GSI and specific to each geomechanical unit (HB-GG).

The percentage of match between the theoretical wellbore analysis and the actual well conditions for each method is shown in this figure. According to this figure, the match percentage under intact rock conditions for the two cases HB-IT and HB-IG are 37.5% and 49.6%, respectively. This percentage for the values of m and s obtained from RMR in the two cases HB-RT and HB-RG is 61.8% and 70.2%, respectively. Additionally, this percentage for the values of m and s obtained from GSI in the two cases HB-GT and HB-GG is 62% and 68.3%, respectively. As a result, considering parameters for geomechanical units and assuming rock mass conditions improves the accuracy of the analytical model.

A back-analysis was conducted using sensitivity analysis to determine the optimal values for *m* and *s* in the Hoek-Brown criterion, aiming to achieve the highest agreement between the results of the theoretical analysis and wellbore observations. The results of the back-analysis for various m and s values are presented in **Figure 8**. The back-analysis indicates that the increase in accuracy and agreement is more dependent on the value of *m*. The optimal range for *m* is between 12 and 20, while the optimal value for *s* is between 0.6 and 1. Choosing the best values for *m* and *s* increases the agreement between predicted and observed wellbore failures to 68%. The corresponding optimal values for *m* and *s* are 16 and 1, respectively.

7. Conclusions

In this study, the parameters used in the Hoek-Brown criterion for assessing wellbore instability were examined by identifying wellbore discontinuities and defining geomechanical units. The hierarchical clustering method showed higher accuracy in defining geomechanical units compared to density-based and K-means methods. Among the clustering methods, the least variance method with the standard Euclidean metric had the highest correlation with segmented plugs (94%) and a silhouette index of 0.48. The distribution of discontinuities indicates that lamination, bedding, and fractures were more frequently observed in geomechanical units with weaker mechanical properties. The most open fractures were found in geomechanical unit V, which had higher strength due to its dolomitic structure and low porosity. If mechanical properties of the discontinuity surfaces were available, it would be possible to compare modelling results assuming fractured intact rock or to construct a representative volume for rock mass modelling.

The Hoek-Brown criterion, based on the two parameters m and s, assuming intact rock, was compared to six criteria: Mohr-Coulomb, Modified Lade, Stassi D'Alia, Mogi-Coulomb, and both inscribed and circumscribed Drucker-Prager. The research findings indicated that

theoretical analysis using the Hoek-Brown criterion under intact rock conditions, without considering geomechanical units (HB-IT), behaves similarly to the circumscribed Drucker-Prager criterion. This implies that most points within the well are assessed as stable, whereas in reality, this is not the case. However, the accuracy of the criterion significantly increases when considering intact rock with the distinction of geomechanical units (HB-GT), effectively identifying instability points in line with actual wellbore events.

The RMR and GSI classification indices were used to estimate the values of m and s for rock mass conditions, differentiated for each geomechanical unit based on the characteristics and frequency of discontinuities. The assigned scores for RMR and GSI ranged from 72 to 82 and 65 to 85, respectively, with the RMR value being slightly higher than GSI. Estimating the values of m and s using RMR and GSI resulted in the theoretical analysis of all wellbore points as unstable, enhancing the accuracy of the Hoek-Brown criterion for this well. Furthermore, when the m and s values were differentiated by geomechanical units for the rock mass (in the HB-RG and HB-GG scenarios), the Hoek-Brown criterion also performed in predicting stable points within the wellbore. The results of back-analysis to find the best m and s values show that the accuracy is more influenced by m than by s. The m values estimated through various methods showed a reasonable agreement with the best m value obtained from back-analysis, while the estimated s values had a greater deviation compared to the best s value from the back-analysis.

The research results indicate that the conditions and parameters used in the Hoek-Brown criterion have a significant impact on the conclusions drawn from this criterion. When applying this criterion under intact rock conditions, all points within the wellbore are predicted to be stable, which represents the lower limit for mud weight. Conversely, when assuming rock mass conditions, most points are predicted to be unstable, indicating the upper limit for mud weight. However, by using geomechanical units and differentiating the parameters, a much closer approximation to a mid-range value can be achieved using this criterion.

Funding

This research received no funding.

8. References

Abazari, F., Jalilifar, H., & Riahi, M. A. (2022). Evaluation of Wellbore Stability by Analytical and Numerical Methods: A Case Study in a Carbonate Oil Field. *Earth and Planetary Science, 1*(1), 10-21.

Abbas, O. A. (2008). Comparisons between data clustering algorithms. *International Arab Journal of Information Technology (IAJIT), 5*(3).

Abdideh, M., & Navadeh Tayyebi, M. (2020). Application of Quantitative Risk Assessment in Wellbore Stability Analysis of Directional Wells. *Journal of Petroleum Science and Technology, 10*(4), 2-9.

Abdollahipour, A., Soltanian, H., Pourmazaheri, Y., Kazemzadeh, E., & Fatehi-Marji, M. (2019). Sensitivity analysis of geomechanical parameters affecting a wellbore stability. *Journal of Central South University, 26*(3), 768-778.

Aboutaleb, S., Behnia, M., Bagherpour, R., & Bluekian, B. (2018). Using non-destructive tests for estimating uniaxial compressive strength and static Young's modulus of carbonate rocks via some modeling techniques. *Bulletin of Engineering Geology and the Environment, 77*, 1717-1728.

Agheshlui, H., & Matthai, S. (2017). Uncertainties in the estimation of in situ stresses: effects of heterogeneity and thermal perturbation. *Geomechanics and Geophysics for Geo-energy and Geo-resources, 3*(4), 415-438.

Al-Ajmi, A. M., & Zimmerman, R. W. (2005). Relation between the Mogi and the Coulomb failure criteria. *International Journal of Rock Mechanics and Mining Sciences, 42*(3), 431-439.

AL-Kaaby, L. F., Rashidi, S., Ghamarpoor, R., Hosseini, S., Al-Saedi, H. N., & Golab, E. G. (2024). Determining the geomechanical units using rock physics methods. *Petroleum Research*.

Anemangely, M., Ramezanzadeh, A., & Behboud, M. M. (2019). Geomechanical parameter estimation from mechanical specific energy using artificial intelligence. *Journal of Petroleum Science and Engineering, 175*, 407-429.

Asaka, M., & Holt, R. M. (2021). Anisotropic wellbore stability analysis: Impact on failure prediction. *Rock Mechanics and Rock Engineering, 54*(2), 583-605.

Azadpour, M., Manaman, N. S., Kadkhodaie-Ilkhchi, A., & Sedghipour, M.-R. (2015). Pore pressure prediction and modeling using well-logging data in one of the gas fields in south of Iran. *Journal of Petroleum Science and Engineering, 128*, 15-23.

Bienawski, Z. (1976). Rock mass classifications in rock engineering.

Brown, E., & Hoek, E. (1980). *Underground excavations in rock*: CRC Press.

Dalirnasab, A., Marji, M. F., Nejati, H. R., & Mohebi, M. (2024). Effects of porosity on the strength and mechanical behaviour of porous geo-materials under cyclic loading: Mechanics of Porous Geo-Materials. *Rudarsko-geološko-naftni zbornik, 39*(2), 15-30.

Edimann, K., Somerville, J., Smart, B., Hamilton, S., & Crawford, B. (1998). *Predicting rock mechanical properties from wireline porosities.* Paper presented at the SPE/ISRM Rock Mechanics in Petroleum Engineering.

Elyasi, A., & Goshtasbi, K. (2015). Using different rock failure criteria in wellbore stability analysis. *Geomechanics for Energy and the Environment, 2*, 15-21.

Ewy, R. T. (1999). Wellbore-stability predictions by use of a modified Lade criterion. *SPE Drilling & Completion, 14*(02), 85-91.

Farquhar, R., Somerville, J., & Smart, B. (1994). *Porosity as a geomechanical indicator: an application of core and log*

data and rock mechanics. Paper presented at the SPE Europec featured at EAGE Conference and Exhibition.

Fjaer, E., Holt, R., Horsrud, P., Raaen, A., & Risnes, R. (2008). Geological aspects of petroleum related rock mechanics. *Developments in petroleum science, 53*, 103-133.

Garavand, A., Stefanov, Y. P., Rebetsky, Y. L., Bakeev, R. A., & Myasnikov, A. V. (2020). Numerical modeling of plastic deformation and failure around a wellbore in compaction and dilation modes. *International Journal for Numerical and Analytical Methods in Geomechanics, 44*(6), 823-850.

Gharechelou, S., Amini, A., Bohloli, B., Tavakoli, V., Ghahremani, A., & Maleki, A. (2022). An integrated geomechanical model for a heterogeneous carbonate reservoir in SW Iran, using geomechanical unit concept. *Bulletin of Engineering Geology and the Environment, 81*(7), 268.

Gholami, R., Moradzadeh, A., Rasouli, V., & Hanachi, J. (2014). Practical application of failure criteria in determining safe mud weight windows in drilling operations. *Journal of Rock Mechanics and Geotechnical Engineering, 6*(1), 13-25.

Hasan, M. M. U., Hasan, T., Shahidi, R., James, L., Peters, D., & Gosine, R. (2023). Lithofacies identification from wireline logs using an unsupervised data clustering algorithm. *Energies, 16*(24), 8116.

Heydari Gholanlo, H., & Nikkhah, M. (2023). Active Fault Detection by an Automatic Breakout Geometry Characterization Algorithm from Ultrasonic Borehole Imager. *SPE Reservoir Evaluation & Engineering, 26*(03), 565-576.

Hoek, E. (1994). Strength of rock and rock masse.

Hoek, E., & Brown, E. (1988). *The Hoek-Brown failure criterion–a 1988 update.* Paper presented at the Proc. 15th Can. Rock Mech. Symp, Toronto, Canada.

Hoek, E., & Brown, E. (2019). The Hoek–Brown failure criterion and GSI–2018 edition. *Journal of Rock Mechanics and Geotechnical Engineering, 11*(3), 445-463.

Hudson, J. A., & Harrison, J. P. (2000). *Engineering Rock Mechanics: An Introduction to the Principles*: Elsevier Science.

Jaeger, J. C., Cook, N. G. W., & Zimmerman, R. (2007). *Fundamentals of Rock Mechanics*: Wiley.

Jamshidi, E., & Amani, M. (2014). Numerical wellbore stability analysis using discrete element models. *Petroleum Science and Technology, 32*(8), 974-982.

Jearsiripongkul, T., Keawsawasvong, S., Thongchom, C., & Ngamkhanong, C. (2022). Prediction of the stability of various tunnel shapes based on Hoek–Brown failure criterion using artificial neural network (ANN). *Sustainability, 14*(8), 4533.

Kadkhodaie, A. (2021). The impact of geomechanical units (GMUs) classification on reducing the uncertainty of wellbore stability analysis and safe mud window design. *Journal of Natural Gas Science and Engineering, 91*, 103964.

Kang, K.-S., Hu, N.-L., Sin, C.-S., Rim, S.-H., Han, E.-C., & Kim, C.-N. (2017). Determination of the mechanical parameters of rock mass based on a GSI system and displacement back analysis. *Journal of Geophysics and Engineering, 14*(4), 939-948.

Kang, Y., Yu, M., Miska, S., & Takach, N. E. (2009). *Wellbore stability: A critical review and introduction to DEM.* Paper presented at the SPE Annual Technical Conference and Exhibition?

Klemme, H. D. (1984). *Oil and gas maps and sections of the Arabian-Iranian basin* (2331-1258). Retrieved from

Lakirouhani, A., Bahrehdar, M., Medzvieckas, J., & Kliukas, R. (2021). Comparison of predicted failure area around the boreholes in the strike-slip faulting stress regime with Hoek-Brown and Fairhurst generalized criteria. *Journal of Civil Engineering and Management, 27*(5), 346-354.

Ma, T., Yang, Z., & Chen, P. (2018). Wellbore stability analysis of fractured formations based on Hoek-Brown failure criterion. *International Journal of Oil, Gas and Coal Technology, 17*(2), 143-171.

Mehrabian, A. (2016). The stability of inclined and fractured wellbores. *SPE Journal, 21*(05), 1518-1536.

Mehrgini, B., Memarian, H., Dusseault, M. B., Eshraghi, H., Goodarzi, B., Ghavidel, A., . . . Hassanzadeh, M. (2016). Geomechanical characterization of a south Iran carbonate reservoir rock at ambient and reservoir temperatures. *Journal of Natural Gas Science and Engineering, 34*, 269-279.

Nazari Sarem, M., & Riahi, M. A. (2020). Geomechanical unit modeling using seismic and well log data in one of the southwestern Iranian oilfields. *Journal of Petroleum Exploration and Production Technology, 10*(7), 2805-2813.

Ostadhassan, M. (2016). Geomechanics and elastic anisotropy of shale formations. In *New Frontiers in Oil and Gas Exploration* (pp. 165-207): Springer.

Pašić, B., Gaurina Međimurec, N., & Matanović, D. (2007). Wellbore instability: causes and consequences. *Rudarsko-geološko-naftni zbornik, 19*(1), 87-98.

Pourreza, S., Hajizadeh, F., & Kadkhodaie, A. (2023). Estimation of geomechanical units using petrophysical logs, core and supervised intelligent committee machine method to optimize exploration drilling operations. *Arabian Journal of Geosciences, 16*(3), 149.

Prakash, S. (2024). Segregation of rock properties using machine learning algorithm with Euclidean distance. *International Journal of Mining and Mineral Engineering, 15*(1), 71-90.

Rafiei Renani, H., & Cai, M. (2022). Forty-year review of the Hoek–Brown failure criterion for jointed rock masses. *Rock Mechanics and Rock Engineering, 55*(1), 439-461.

Rahimi, R., & Nygaard, R. (2015). Comparison of rock failure criteria in predicting borehole shear failure. *International Journal of Rock Mechanics and Mining Sciences, 79*, 29-40.

Rahimi, R., & Nygaard, R. (2018). Effect of rock strength variation on the estimated borehole breakout using shear failure criteria. *Geomechanics and Geophysics for Geo-energy and Geo-resources, 4*, 369-382.

Ruiz, M. L. C., & Batezelli, A. (2024). Correlation between geomechanical and sedimentary facies and their implications for flow unit definition in the pre-salt carbonate reservoir, Brazil. *Journal of South American Earth Sciences, 141*, 104958.

Stassi-D'Alia, F. (1967). Flow and fracture of materials according to a new limiting condition of yelding. *Meccanica, 2*, 178-195.

Suchowerska, A. M., Merifield, R. S., Carter, J. P., & Clausen, J. (2012). Prediction of underground cavity roof collapse

using the Hoek–Brown failure criterion. *Computers and Geotechnics, 44*, 93-103.

Tavakoli, V. (2015). Chemostratigraphy of the Permian–Triassic strata of the offshore Persian Gulf, Iran. In *Chemostratigraphy* (pp. 373-393): Elsevier.

Tavakoli, V., Naderi-Khujin, M., & Seyedmehdi, Z. (2018). The end-Permian regression in the western Tethys: sedimentological and geochemical evidence from offshore the Persian Gulf, Iran. *Geo-Marine Letters, 38*, 179-192.

Veeken, C., Walters, J., Kenter, C., & Davies, D. (1989). *Use of plasticity models for predicting borehole stability.* Paper presented at the ISRM International Symposium.

Wang, Z., Wang, T., Wang, W., & Zhang, Z. (2023). Size of representative elementary volume for heterogeneous rocks evaluated using distinct element method. *Acta Geotechnica, 18*(4), 1883-1900.

Wei, X., Zuo, J., Shi, Y., Liu, H., Jiang, Y., & Liu, C. (2020). Experimental verification of parameter m in Hoek–Brown failure criterion considering the effects of natural fractures. *Journal of Rock Mechanics and Geotechnical Engineering, 12*(5), 1036-1045.

Yamashiro, Y., Yasuda, T., Chiam, S., & Lim, Y. (2018). *Proposed Approach of Rock Mass Classification and Hoek-Brown Strength Parameters in Singapore.* Paper presented at the ISRM International Symposium-Asian Rock Mechanics Symposium.

Yang, B., & Elmo, D. (2022). Why engineers should not attempt to quantify GSI. *Geosciences, 12*(11), 417.

Yang, X. L., Li, L., & Yin, J. H. (2004). Stability analysis of rock slopes with a modified Hoek–Brown failure criterion. *International Journal for Numerical and Analytical Methods in Geomechanics, 28*(2), 181-190.

Zadravec, D., & Krištafor, Z. (2018). Contribution to the methodology of determining the optimum mud density-a case study from the offshore gas condensate field D in the Persian Gulf. *Rudarsko-geološko-naftni zbornik, 33*(4).

Zeynali, M. E. (2012). Mechanical and physico-chemical aspects of wellbore stability during drilling operations. *Journal of Petroleum Science and Engineering, 82*, 120-124.

Zhang, J., Lang, J., & Standifird, W. (2009). Stress, porosity, and failure-dependent compressional and shear velocity ratio and its application to wellbore stability. *Journal of Petroleum Science and Engineering, 69*(3-4), 193-202.

Zhang, L., Cao, P., & Radha, K. (2010). Evaluation of rock strength criteria for wellbore stability analysis. *International Journal of Rock Mechanics and Mining Sciences, 47*(8), 1304-1316.

Zhou, S. (1994). A program to model the initial shape and extent of borehole breakout. *Computers & Geosciences, 20*(7-8), 1143-1160.

Zoback, M. D. (2010). *Reservoir geomechanics*: Cambridge university press.

Zuo, J.-p., Li, H.-t., Xie, H.-p., Ju, Y., & Peng, S.-p. (2008). A nonlinear strength criterion for rock-like materials based on fracture mechanics. *International Journal of Rock Mechanics and Mining Sciences, 45*(4), 594-599.

SAŽETAK

Analiza stabilnosti kanala bušotine na temelju Hoek-Brownova kriterija loma korištenjem geomehaničkih jedinica i procjene diskontinuiteta

Točnost procjene stabilnosti kanala bušotine postaje pouzdana kada se koristi dovoljno podataka geomehaničkoga modela i odgovarajući kriteriji za predviđanje loma stijena. U analizi stabilnosti kanala bušotine često se koristi Hoek-Brownov kriterij; međutim, malo je pozornosti posvećeno određivanju parametara i specifičnih uvjeta za njegovu primjenu (netaknuta stijena ili stijenska masa) unutar bušotina. U ovome je radu provedena teorijska analiza stabilnosti kanala bušotine primjenom raznih kriterija za predviđanje loma stijena s primarnim fokusom na usporedbu Hoek-Brownova kriterija za uvjete netaknute stijene ili stijenske mase. Razvijen je geomehanički model korištenjem rezultata petrofizičkih svojstava stijena, laboratorijskih testova i karotažnih mjerenja u bušotinama. Geomehaničke jedinice kanala bušotine određene su primjenom klasterskih algoritama, uz podršku sondi u bušotini. Prirodni diskontinuiteti unutar bušotine utvrđeni su snimanjem stijenki kanala bušotine (engl. *image logs*), a njihova je distribucija mapirana za svaku geomehaničku jedinicu. Parametri za netaknutu stijenu u Hoek-Brownovu kriteriju dobiveni su iz rezultata laboratorijskih testova, dok su oni za uvjete stijenske mase određeni pomoću RMR klasifikacije stijenske mase (engl. *rock mass rating*, RMR) i geološkoga indeksa čvrstoće (GSI). Rezultati pokazuju da primjena Hoek-Brownova kriterija uz pretpostavku netaknute stijene ne pruža pouzdanu procjenu stabilnosti kanala bušotine. Međutim, korištenjem toga kriterija u uvjetima stijenske mase mogu se točno predvidjeti nestabilnosti kanala bušotine s obzirom na uvjete u bušotini. Osim toga, procjena uvjeta u bušotini na temelju geomehaničkih jedinica poboljšava točnost teorijske analize i omogućava identifikaciju stabilnih i nestabilnih zona.

Ključne riječi:
Hoek-Brownov kriterij, geomehanička jedinica, klasifikacija stijenske mase, stabilnost kanala bušotine

Author's contribution

Mohamadali Chamanzad (PhD candidate): data curation, formal analysis, investigation, resources, software, writing – original draft and writing – review & editing. **M. Nikkhah** (Associate Professor at the Faculty of Engineering): conceptualization, formal analysis, methodology, project administration, resources, supervision, validation, visualization and writing – review & editing. **A. Ramezanzadeh** (Professor at the Faculty of Engineering): conceptualization, supervision, validation, visualization, review and editing. **Misha Pezeshki** (Senior Staff of Pars Oil and Gas Company): data curation, supervision, validation, visualization, and review. **Imandokht Mostafavi** (Senior Staff of Pars Oil and Gas Company): data curation, supervision, validation, visualization, and review.
All authors have read and agreed to the published version of the manuscript.